Elastic-Plastic Calculation of a Steel Beam by the Finite Element Method

O. Sucharda, J. Vasek, J. Kubosek

Abstract—The purpose of the paper is to assess behaviour of steel beams during a loading test and the FEM models which take into account computational nonlinearities. The steel beams are loaded with a single load. The calculation was made in ANSYS and vFEM, the own software under development. In case of vFEM which can be used for nonlinear solutions of tasks, the computation and algorithm are supported by examples.

Keywords— Steel beam, 3D isoparametric finite elements, stress strain curve, load deformation diagram, plastic behaviour, load capacity

I. Introduction

STEEL offers good material properties and is suitable for designs and solutions of engineering structures such as ceiling beams, latticework structures, or columns.

The design [1] and analysis of the advanced steel structure is often connected with investigation into behaviour of structural details where strain is concentrated in places where local loads are applied or in places where the cross-section is weaker. This is also the case of structural details [2] and imperfections [3], [4] and [5]. Steel is also frequently combined with other materials, for instance with glass [6] or CFRP reinforcement [7]. This requires a specific approach to the analyses and calculations.

In those cases, the structural optimising should be performed in addition to the standard design and analyses. The analyses deal in most cases with 3D computational models and the physical [8], geometrical [9] or structural nonlinearities which are considered in calculations. Different approaches are available for different structural issues [10]. Certain experiments exist for some structure solutions [11], but they cannot be used in general for other alternatives.

This is, for instance, the case of weakened or reinforced cross-section.

The material and computational models are often simplified in the analyses (1D or 2D) or combined computational models (sub-models) are used [12] or some phenomena are neglected.

In order to understand better the behaviour of structural details and selection of the optimum construction, it is recommended to focus not only on one type of the structural solution. Attention should be paid to the behaviour of steel beams without any adaptations with a reinforced/weakened cross-section. And this is the key topic discussed by this article which describes and evaluates some experiments of steel beams as well as numerical analyses based on the 3D computational and material models. Software such as (ANSYS [13], SCIA [14]) can be used for calculations. In many cases, it is, however, inefficient to use them. Or it is too demanding or impossible because of a locked source code or commercial nature of the software. Therefore, a better solution would be to use the own computational software applications developed in Matlab [15] or in similar development environment. When designing and optimising the structural solution, it is advisable to include into the calculation the real character of input data: a different strength or homogeneity of materials [16], [17] and [18].

The purpose of the paper is to assess behaviour of steel beams during a loading test and the 3D models [19] which take into account computational nonlinearities [20]. The calculation was performed in the academic developed software vFEM. Calculations are also performed in ANSYS.

In case of the own software in vFEM which can be used to calculate the nonlinear solution, the computation and algorithm are supported by examples.

II. Computational Tools

Several computational tools are available for the design and analyses of the steel structures. In particular, strain and stress in the structure are taken into account.

Most computational tools and computational algorithms are based on the Finite Element Method. This methods ranks among the numerical methods and is based on discretising of a computational model into small segments for which an approximate solution is searched. The small segments are referred to as the finite elements and their basic parameters are the base function and shape. A finite element can be a beam, 2D or 3D element. In the basic approach the linear FEM solution is employed where the matrix equation is:

O. Sucharda is with the Department of Structural Mechanics, Faculty of Civil Engineering, VSB Technical University of Ostrava (email:oldrich.sucharda@vsb.cz).

J. Vasek was with the Department of Structural Mechanics, Faculty of Civil Engineering, VSB Technical University of Ostrava (email:oldrich.sucharda@vsb.cz).

J. Kubosek is with the Department of Structural Mechanics, Faculty of Civil Engineering, VSB Technical University of Ostrava (email:oldrich.sucharda@vsb.cz).

$$\mathbf{Ku} = \mathbf{F}, \tag{1}$$

where K is the stiffness matrix of the structure, u is the unknown vector of displacement and F is the load vector.

This method is used in ANSYS as well as in the software application which is being developed in Matlab – vFEM. A typical construction task is used in order to illustrate two finite elements implemented in the software. It is a tetrahedron with four nodes and one integration point and an isoparametric finite element with eight integration points. Fig. 1 shows the finite elements. The isoparametric finite element is calculated using the Jacobi transformation. In particular, it is based on an 3D 8 node isoparametric finite element. The base functions of the element are described in (2).

$$N_{(\eta,\xi,\zeta)} = \frac{1}{8}(1+\eta\eta_i)(1+\xi\xi_i)(1+\zeta\zeta_i) \tag{2}$$

The author used the tetrahedron as a finite element, for instance, in [21].
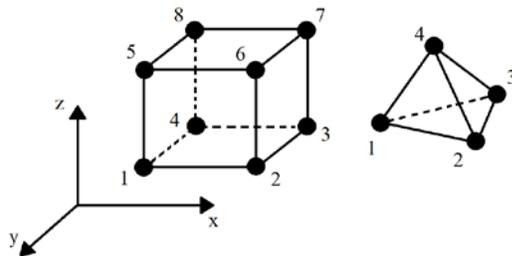
Fig. 1 8-node (brick) element, 4-node element in 3D

A. Numerical example – Cantilever

An elastic analysis of the bracket was carried out as correction of the computational model. Two types of calculations have been carried out. The only difference in the structural geometry was the cross-section of the element (Fig. 2). In the first case, the rectangular cross section 0.16 m x 0.074 m has been chosen. In the second case, the sample was a steel rolled profile, IPN 160.
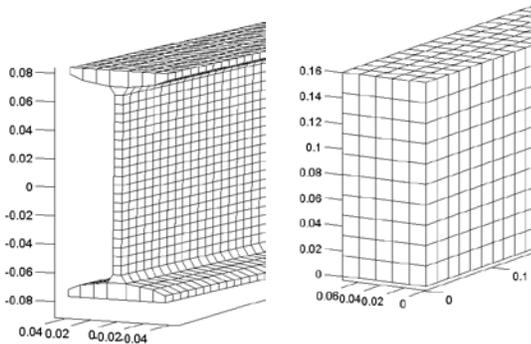
Fig. 2 meshing for 8-node element (IPN 160 – left, rectangular - right)

The length of the cantilever beam is 1 m. It is loaded with a single force of 10 kN at the loose end. A beam model and 3D finite models (4 node, isoparametric and 8 node elements) were used.

Cross-section	stress deflection	Bar	4 node	8 node
Rectangle	[MPa]	31.67	28.93	30.57
	[mm]	0.63	0.63	0.63
IPN 160	[MPa]	85.47	82.84	83.22
	[mm]	1.70	1.85	1.83

Table 1. comparison of the stress and deformation at the beam bracket for different computational models
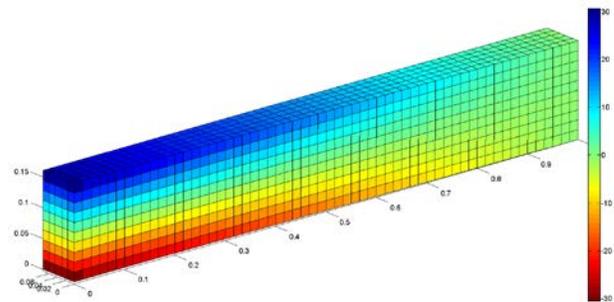
Fig. 3 stress σ_x [MPa] for the 8 node element, deformed cantilever, cross-section rectangular (0.16 m x 0.074 m), load 10 kN
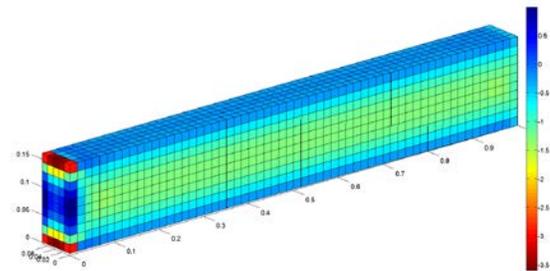
Fig. 4 stress τ_{xz} [MPa] for the 8 node element, deformed cantilever, cross-section rectangular (0.16 m x 0.074 m), load 10 kN
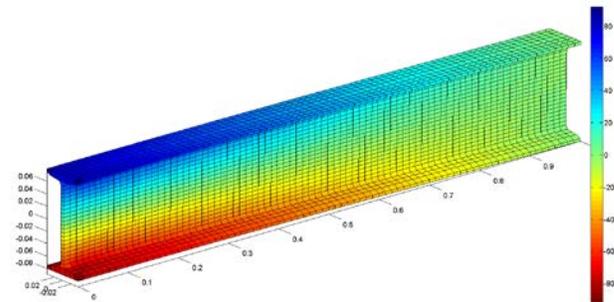
Fig. 5 stress σ_x [MPa] for the 8 node element, deformed cantilever beam, cross-section IPN160, load 10 kN

Fig. 3 and 4 show the normal and shear stress for the first case, while Fig. 5 and 6 shows the second case.

Table 1 lists the results: the deformation in the loading direction as well as the maximum stress in the fixing point.
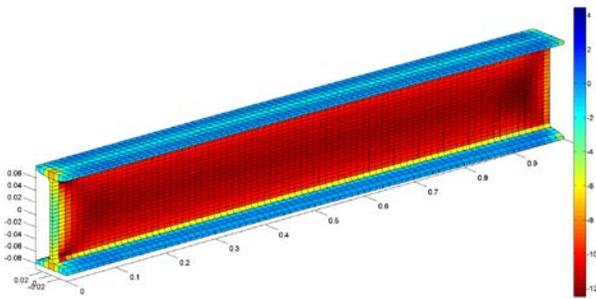
Fig. 6 stress τ_{xz} [MPa] for the 8 node element, deformed cantilever beam, cross-section IPN160, load 10 kN

The values indicate that the difference between the stresses and deformations is not more than 7 per cent. For such values, it is advisable to consider suitable setup of the input parameters in the model, for instance, a finite element mesh. Such setup has been also considered in further calculations.

B. Modeling of support cantilever

Stress values in edges of flange are expressed according to the equation (3). Limit value of normal stress is $\sigma_x = 85.47\ MPa$. This result corresponds with calculated value in FEM model.

$$\sigma_x = \frac{M_Y}{W_{Y,el}} \qquad (3)$$

The Tab. 2 shows maximum normal stresses σ_x for *10 kN* load in cantilever. Stresses were evaluated as mean value from results calculated in edge elements on flange. The similar stress as calculated according to the equation (3) exhibit variant with supports divided into all nodes in cantilever. A result for this variant is shown in figure 5. Normal stress takes the value $\sigma_x = 83.22\ MPa$. The highest difference was calculated for variant with one node support. This is due to concentration of stress in neighborhood of a node. From other considered options better reflects cantilever support flanges. This type of support can be interpreted as a pair of forces. It symbolized bending moment (dominant reaction in restrain).

Support	All cross-section	Axis	Web	Flange
σ_x **[MPa]**	83.22	411.84	138.34	109.23

Table 2. Comparing of stress for different types of support

III. NONLINEAR ANALYSIS

A. Nonlinear solver

In the nonlinear analysis, the stiffness matrix of the structure obtained from (1) is not constant any more but is a function of nodal dislocations. The set of nonlinear equations is then:

$$\mathbf{K(u)u} = \mathbf{F} \ . \qquad (4)$$

Where **K** is the stiffness matrix of the structure which depends on the load and displacement vector. The nonlinear set of equations can be solved approximately only. The Newton-Raphson method was used in vFEM.

It is based on calculation of unbalanced forces. As errors do not cumulate during the calculation, it is not necessary to calculate the task again. The approach is based on the Euler method where the calculation is divided into loading steps:

$$\mathbf{K(u)}\Delta\mathbf{u}_i = \Delta\mathbf{F}_i, \qquad (5)$$

Where $\mathbf{K(u)}$ is the stiffness matrix which depends on the dislocation factor **u**, $\Delta\mathbf{u_i}$ is an increment in strain for the loading step $\Delta\mathbf{F_i}$.

The assumption is the balanced condition

$$\mathbf{f_{ext}} - \mathbf{f_{int}} = \mathbf{0} \ , \qquad (6)$$

where f_{ext} is a vector of external forces and f_{int} is the vector of internal forces. For the nonlinear calculation, the stiffness matrix $K(u)$ changes into K'. In a certain loading step (iteration) the balanced condition ceases to exist and the residual vector is created:

$$\mathbf{f}_{ext} - \mathbf{f}_{int} = \mathbf{g} \ . \qquad (7)$$

A deformation increment, $\Delta\mathbf{\alpha}$, resulting from the residual vector is solved using:

$$\mathbf{K'}\Delta\mathbf{\alpha} = \mathbf{g} \ . \qquad (8)$$

It is also necessary to create a new stiffness matrix and to calculate a new residual vector. The calculation is repeated until the residual vector is zero or until the required accuracy is reached. In that loading step, the calculation is finished.

Then, a new loading step $\Delta\mathbf{F}_{i+1}$ is used and the process is repeated. The calculation is over once the required load is obtained. Sometimes, the calculation can end before the required load is reached. This is, for instance, the situation when the new balanced condition can be found for the structure.

B. The material model of steel

Steel is an isotropic material with a high strength. The compressive strength and tensile strength are same. Typically, the strength is between 300 MPa to 700 MPa. It follows from the strain stress curve in Fig. 7a that behaviour of the steel is, at the beginning, linearly elastic. The linear elasticity exists up to the level which is identified as the limit of proportionality. An important value is the yield point - if it is exceeded, plastic deformations appear. The stress-strain curve beyond the yield point depends on a specific composition of the steel, working

procedure, technology adaptations or the selected degree of idealisation.
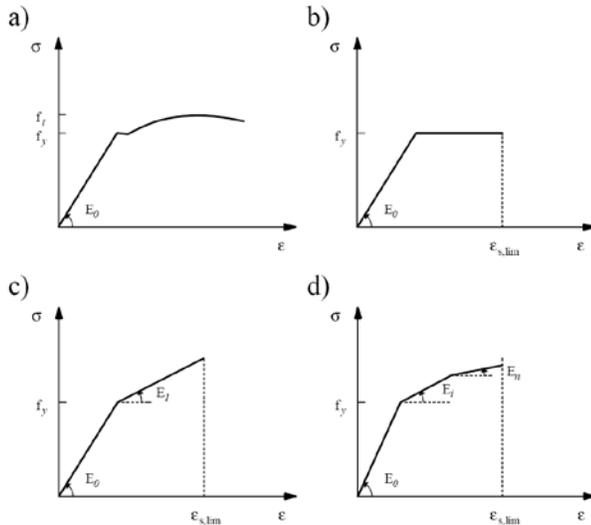
Fig. 7 stress-strain diagram a) structural steel b) the ideal elastic-plastic behaviour c) the ideal elastic-plastic behaviour with linear hardening d) the multilinear behaviour

Fig. 7 shows the idealised stress-strain diagrams for design of structure. These are the linear elastic, ideal elastic-plastic, ideal elastic-plastic behaviour with linear hardening and multilinear stress-strain diagram. It is recommended to use the ideal elastic-plastic stress-strain curve or an elastic-plastic stress-strain diagram with linear hardening.

This diagram requires good information about the yield point, initial modulus of elasticity, the modulus of elasticity for the hardening, and the maximum relative deformation. The condition of elasticity for the single-axis state of stress in the elastic-plastic stress-strain diagrams simplifies the expression as follows:

$$\sigma \leq f_y, \qquad (9)$$

where σ is stress for the single-axis state of stress and f_y is The relative deformation is limited by $\varepsilon_{s,lim}$. Because this is a 3D task, it is necessary to define a condition of plasticity for the space. The HMH condition was chosen for that purpose.

For the other calculations and vFEM, an ideal elastic-plastic model of steel was chosen. The final theoretical matrix of stiffness of the elastic-plastic material is as follows:

$$\mathbf{D_{ep}} = \mathbf{D_e} - \frac{\mathbf{D_e}\left\{\dfrac{d\mathbf{f}}{d\boldsymbol{\sigma}}\right\}\left\{\dfrac{d\mathbf{f}}{d\boldsymbol{\sigma}}\right\}^T \mathbf{D_e}}{\left\{\dfrac{d\mathbf{f}}{d\boldsymbol{\sigma}}\right\}^T \mathbf{D_e}\left\{\dfrac{d\mathbf{f}}{d\boldsymbol{\sigma}}\right\} - \psi\sqrt{\left\{\dfrac{d\mathbf{f}}{d\boldsymbol{\sigma}}\right\}^T \left\{\dfrac{d\mathbf{f}}{d\boldsymbol{\sigma}}\right\}}}. \qquad (10)$$

In that case a possibility would be to use a zero stiffness matrix for the calculation and algorithmising of the ideal elastic-plastic material. The result might be that the set of equations become singular in places where plasticising clusters occur.

For those reason the computational process should be such so that algorithms, could be developed easily. The calculation uses the small material stiffness which is defined by an auxiliary parameter

$$\rho = \frac{E_1}{E_0}, \qquad (11)$$

where E_1 is the small material stiffness for calculation and E_0 is the material stiffness of structural steel. The new stiffness of the finite element is considerably lower than the original stiffness. It is not, however, zero. Because the stiffness decreases, ρ ranges between 1 and 0. Below are more details about ρ. The parameters influence, in particular, the rate of convergence for iterations.

IV. EXPERIMENT

In order to support and validate the numerical calculations, an experiment was performed: This was a three-point bending test of a steel beam, IPN160. The test was carried out in the laboratory of Building Materials, at VŠB - Technical University of Ostrava.

The purpose was to monitor the loading process, the principle of failure and the stress-strain curve. The obtained data were used for validation of the numerical analysis in ANSYS and vFEM (the software under development). Fig. 8 shows the process of the experiment. Two tests were carried out. In Fig. 9 there is a typical breakdown.

Fig. 8 three-point bending test on IPN 160 – experiment.

Fig. 9 failure in the beam - web buckling.

Fig. 10 shows the load-displacement diagram with the loading process.
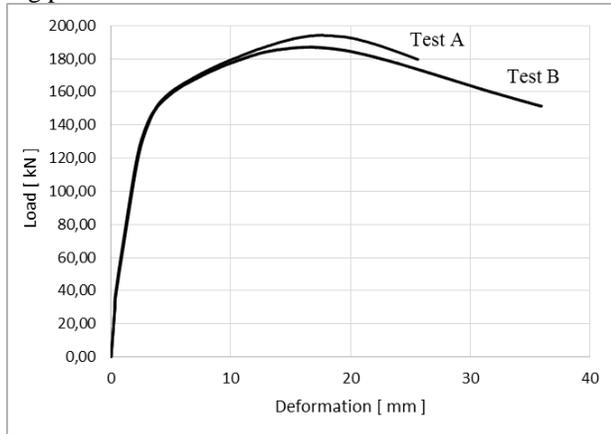
Fig. 10 beam failure - web buckling.

The progress of the both tests is very similar. There is a minor change in the total load capacity and in the descending branch.

V. NONLINEAR ANALYSIS

The software has been used to analyses the loading curve in a three-point bending test of a steel beam. The three-point bending test is applied to a plain beam which is loaded in the middle of its span with a single load. The steel grade is S235 and the cross-section is IPN 160. The distance between the supports is *0.9 m*. For the layout see Fig. 11.
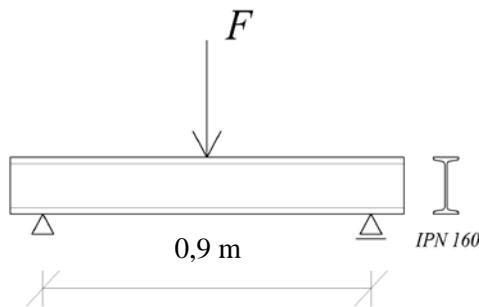
Fig. 11 the structure under modelling.

As this is a 3D model, the position of the loading force and the supports is chosen in line with reality.

The load is applied along the line on the flange width. The supports are located in a line, along the lower flange.

First, the numerical analyses were performed in the new software under development. Then, ANSYS was used for validation.

A. The parametric study for ρ

The parametric study ρ for was performed in order to understand better the elastic-plastic calculation.

As described above, the correct value of ρ needs to be determined in order to obtain correct convergence of the calculation. A parametric study has been created for the convergence parameters and the load curve has been monitored for different values of that parameters. The convergence parameter changed from $1.0e^{-1}$ to $1.0e^{-4}$. Fig. 12 shows the calculated curves.
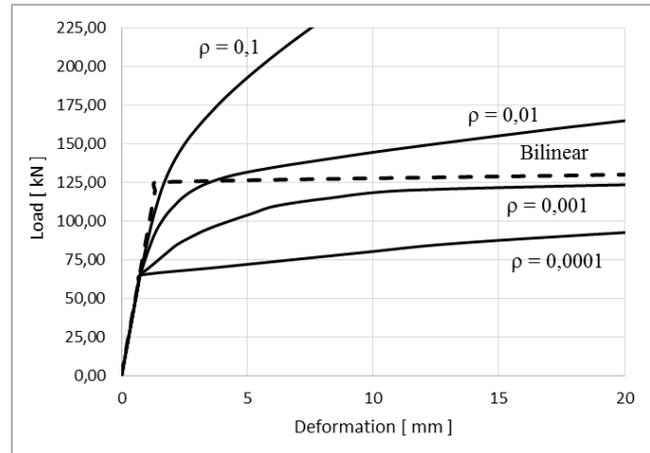
Fig.12 load curves for various convergence parameter.

The chart above contains, in addition to the load curve, the elasticity (bilinear) load curve (the dash line curve). The curves suggest that the nearest convergence towards the bilinear solution should be reached for $\rho = 0.001$. For that value, the first plastic areas appear approximately in the half of the linear area. If compared with the other curves, the convergence is, however, the nearest one to the value resulting from the elasticity analysis.

Parameter ρ	0.1	0.01	0.001	0.0001
Number of iterations	80	36	27	21

Table 3. influence of on the calculation rate

It follows from the chart that the lower ρ is, the more drammatic increase in deformation is with lower load increments. The lower ρ requires less iteration steps in order to obtain the results. The table 3 above shows dependence of the iteration steps on ρ.
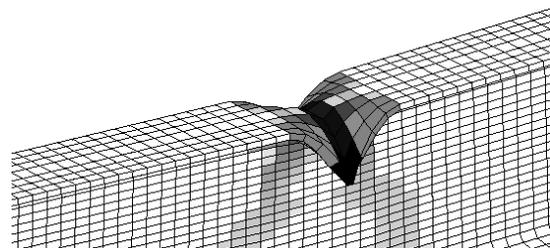
Fig. 13 progress of plasticizing. Dark parts of the beam plasticize with the lower load. Point of the loading force.

B. Limit stress

An important parameter which influences the calculation is the limit stress. This is the stress which, if exceeded, cause the material to plasticize. In case of steel, the limit stress is often represented by the yield point. For S235 the yield point is $f_y=235$ MPa. Several calculations with different limit values have been carried out for the structure. Fig. 13 shows the progress of plasticizing.

The reason was the comparison between the calculated values and the values measured in the experiment. The yield point for S235 is determined by the 5 per cent quantile. For steel of that grade, the limit stress is considerably higher that the specified stress.
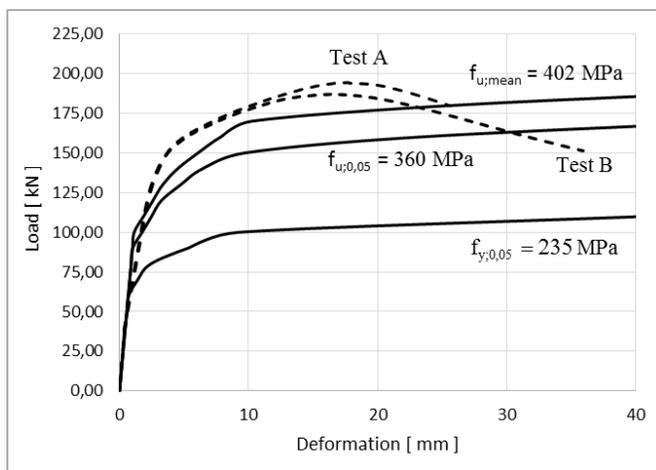
Fig. 14 load curves for different values of the limit stress

Fig. 14 shows the load curves for different values of the limit stress. For the sake of clarity, the A test and the B test is shown in the chart. The chart in Fig. 14 shows, in addition to the load curve, the load chart obtained from a three-point bending test of a steel beam.

Next curves symbolize results from numerical models. The different between models is in limit stress. For the first case was limit stress set up on yield stress *235 MPa*. The first change of stiffness of construction was recognized for smaller deflection and load capacity was about *115 kN*. It means, that yield stress as limit stress for calculation reflecting parameter ρ is extremely small.

For this case was generated model with ultimate stress. According to the show results, the calculated values was not achieved. The most adequate value of limit stress was mean value of ultimate stress *402 MPa*.

C. Influence of the support and force

Several fixing alternatives and possible locations of the load force have been also investigated in the three-point model test (Fig. 11). For those places in the structure, concentration of stress is often an issue. Therefore, results might be unreliable and reality might be described incorrectly.

Different fixing and load alternatives, both in single cases and combinations, have been evaluated for the beam. In the first alternative, the loading force was divided along the flange width into one row. In another alternative, the loading force was divided into three rows – this increased the loading area and reduced local impacts of the load.
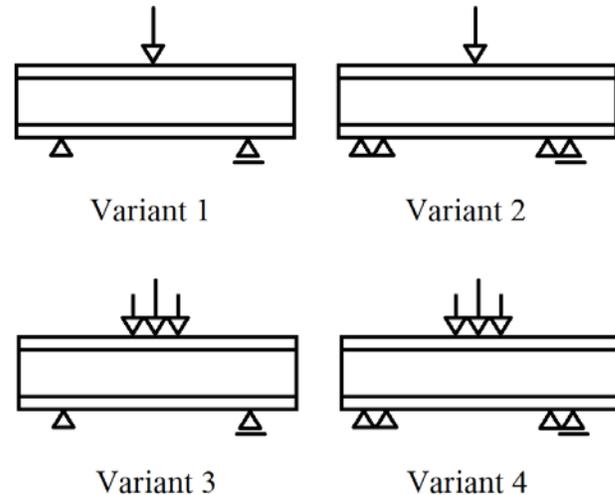
Fig. 15 different supports and loads in the structure model

The supports were located in a line along the flange width. In one alternative, the support was modelled in one line only, while the second alternative used a pair of the line supports.
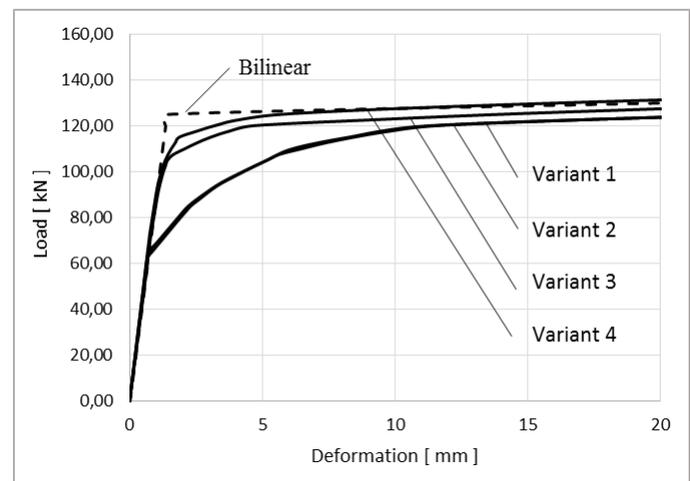
Fig. 16 influence of the location of the supports and load on the loading process

It follows from the chart (Fig. 16) above that the location of the support plays a little role only for the load capacity and deformation which depend on the load. On the other hand, distribution of the load is significant. If the load is distributed into several nodes of the finite element mesh, the maximum increase in the load is achieved. Another factor which has been influenced is the increase in the elastic area of the structure. The first plasticizing of the material occurs with the

considerably higher load than in the case when the load had been applied in one row along the beam flange.

D. 4.3 Calculations in ANSYS

The calculations were performed also in ANSYS. A 3D computational model from the finite volume elements was created for the analysis.

Both physical and geometrical nonlinearities were taken into account there. Contact elements were used in places where the boundary conditions existed.

Fig. 17 shows the computational model of the beam.

For the nonlinear solution, two material models were chosen. The multilinear and bilinear strain-stress curves for the steel were used there. The material models were based on the strength and yield point of the steel. Fig. 18 shows the load displacement diagram.
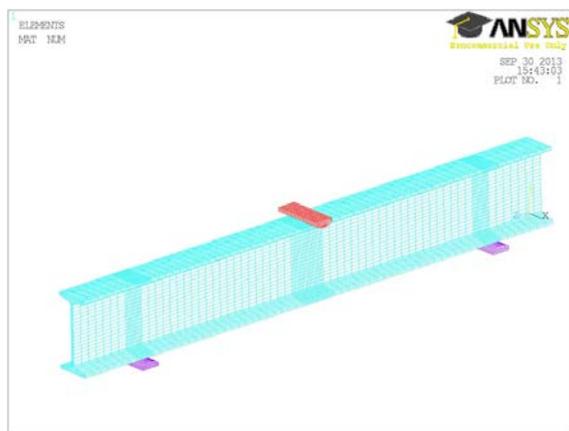
Fig. 17 ANSYS – the FEM mesh in the model
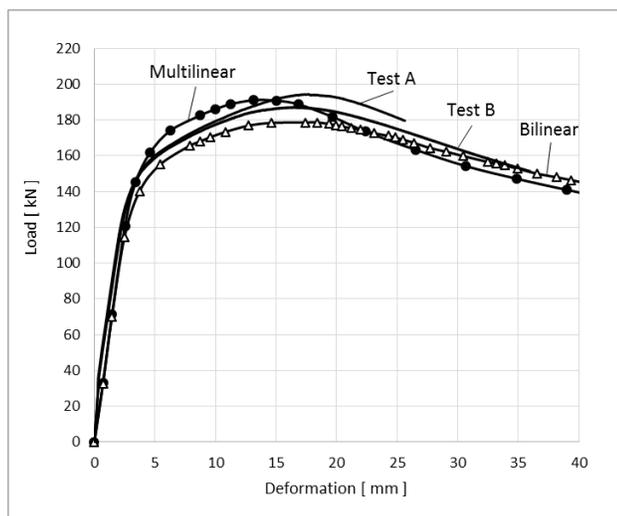
Fig. 18 load-displacement diagram
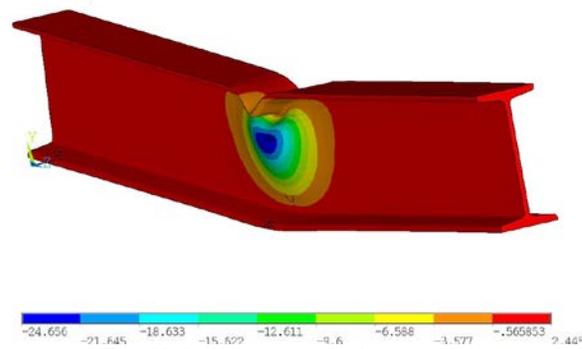
Fig. 19 deformation in the horizontal direction

For the sake of clarity, the graphics in the figure shows the horizontal deformation of the entire model.

VI. CONCLUSION

The paper discussed the approach to the nonlinear analysis of steel structures. The Finite Element Method and 3D computational models were used for this. The computational model of the beam includes the material model of the steel. This system is an elastic-plastic model which is used in the calculation as an auxiliary parameter. 0.001 was chosen as the best value for the model. This value was validated for a steel beam model. The limit stress for the three-point bending test was calculated in the software. The results prove good correlation between the numerical calculation and experiment. Then, the numerical analysis for the experiment was performed in ANSYS. In this case, the stiffness of the beams was slightly overrated in the multilinear stress-strain curve. The reason might be approximation in the stress-strain curve. The paper also discusses impacts of various locations of the supports and load forces. The supports distributed into several nodes in the structure have not had any major impact on the loading process. The load distributed onto a bigger loading area increased slightly the calculated load capacity and, in turn, increased the elastic area of the load curve.

REFERENCES

[1] ČSN EN 1993-1-1. Eurocode 3: Design of steel structures - Part 1-1: General rules and rules for buildings. Praha: ČNI, 2006.

[2] D. Rad. Influence of manufacturing flaws in the truss beams welded joints behaviour. *In AELPS'14, Brasov, Romania, June 26-28, 2014, WSEAS Press*, pp. 13-19. ISBN 978-960-474-386-5.

[3] I. M. Cristutiu, Z. Nagy, Initial imperfection influences on the structural behavior of steel portal frames with variable cross sections and some sustainability considerations-case study. *In 6th WSEAS International Conference on ENERGY, ENVIRONMENT, ECOSYSTEMS and SUSTAINABLE DEVELOPMENT (EEESD '10), Selected Topics in Energy, Environment, Sustainable, Development and Landscaping., WSEAS Press*, pp. 21-32, ISBN 978-960-474-237-0.

[4] XinWu Wang. Nonlinear finite element analysis on the Steel Frame with semi-rigid connections, *7thWSEAS International Conference on Applied Computer and Applied Computational Science,* pp. 31-35, China, April 6-8, 2008

[5] S. Boljanovic, S. Maksimovic, I. Belic, Total fatique life of structural components, *Proceedings of the 2nd WSEAS International Conference on Applied Computer and Theoretical Mechanics,* pp. 1-6, Italy, November 20-22, 2006

[6] O. Pesek, J. Melcher, M. Pilgr, Numerical Analysis of Hybrid Steel-Glass Beam, *In Recent Advances in Engineering, WSEAS Press, 2012*, pp. 234-239, Paris, ISBN 978-1-61804-137-1.

[7] M. Karmazínová, P. Neubauerová, P. Bukovská, Effectiveness of strengthening steel beams using external bonded CFRP lamellas. *In Recent Researches In Engineering Mechanics, Urban & Naval Transportation and Tourism. WSEAS Press*, pp. 243-247, 2012, ISBN 978-1-61804-071-8.

[8] R. Borst, M. Crisfield, ed. Nichtlineare Finite-Elemente-Analyse von Festkörpern und Strukturen, 2014, Berlin. Ernst und Sohn. ISBN 978-3-527-33660-9.

[9] O. Roth, J. Ravinger, Nonlinear interactive buckling solved by FEM. *In Proceedings of the 2nd International Conference on Computational Structures Technology*. Part 1 (of 4); Athens, Greece; Civil-Comp Limited, Edinburgh, United Kingdom. 1994.

[10] K. Seung-Eock, L. Dong-Ho, Second-order distributed plasticity analysis of space steel frames. Engineering Structures 24 (2002) 735–744.

[11] P. Avery, M. Mahendran, Large-scale testing of steel frame structures comprising noncompact sections. Engineering Structures 22 (2000) 920–936.

[12] S. Sreenath, U. Saravanan, V. Kalyanaraman, Beam and shell element model for advanced analysis of steel structural members. Journal of Constructional Steel Research 67 (2011) 1789–1796. doi:10.1016/j.jcsr.2011.05.003

[13] ANSYS, RELEASE 11 DOCUMENTATION FOR ANSYS, SAS IP, INC., 2007.

[14] Scia Engineer [online]. 2012 [cit. 2012-01-01]. Available from WWW: <http://www.scia-online.com>.

[15] MATLAB - The Language of Technical Computing. Software. [on-line]. <http://matlab.com/>. The MathWorks, Inc., Massachusetts, USA, 2014.

[16] T. Vrouwenvelder, The JCSS probabilistic model code. Structural Safety. Vol. 19, Issue 3, pp. 245-251 (7 p). ISSN 0167-4730, 1997.

[17] V. Křivý, P. Marek, Probabilistic design of steel frame structures. Stahlbau. Vol. 76. 2007, Issue 1, Pages 12-20.

[18] M. Krejsa, P. Janas, R. Čajka, Using DOProC Method in Structural Reliability Assessment. *In ICMAM2012, Applied Mechanics and Materiále.* Vol. 300-301 (2013), pp. 860-869 (10 p). ISBN 978-3-03785-651-2. DOI: 10.4028/www.scientific.net/AMM.300-301.860.

[19] R. Kindmann, M. Kraus, Finite-Elemente-Methoden im Stahlbau, 382 pp, Berlin: Ernst & Sohn, 2007, ISBN 978-3-433-01837-8.

[20] J. Ravinger, M. Psotný, Analysis of constructs. Nonlinear problems. Bratislava: STU v Bratislavě, 2007. 174 s. ISBN 978-80-227-2713-6.

[21] O. Sucharda, J. Vasek, D. Mikolasek, Finite Element Analysis of Beam from Rolled IPN 160. *In The 4th International Conference on Green Building, Materials and Civil Engineering. GBMCE 2014*, Taylor & Francis Group. Hong Kong, August 21-22, 2014. (In print).